Available online at www.sciencedirect.com
ScienceDirect
Journal of Environmental Sciences 2011, 23(1) 44–50
JOURNAL OF ENVIRONMENTAL SCIENCES
ISSN 1001-0742
CN 11-2629/X
www.jesc.ac.cn

Application of magnetic particles modified with amino groups to adsorb copper ions in aqueous solution

Yafen Lin[1], Huawei Chen[2], Kaelong Lin[3], Boryann Chen[1], Chyowsan Chiou[3,*]

1. Department of Chemical and Materials Engineering, "National" I-Lan University, I-Lan 260, Taiwan, China. E-mail: yflin@niu.edu.tw
2. Department of Cosmetic Application and Management, St. Mary's Medicine Nursing and Management College, I-Lan 260, Taiwan, China
3. Department of Environmental Engineering, "National" I-Lan University, I-Lan 260, Taiwan, China

Received 09 January 2010; revised 29 March 2010; accepted 29 April 2010

Abstract

A magnetic adsorbent can be easily recovered from treated water by magnetic force, without requiring further downstream treatment. In this research, amine-functionalized silica magnetite has been synthesized using N-[3-(trimethoxysilyl)propyl]-ethylenediamine (TPED) as a surface modification agent. The synthesized magnetic amine adsorbents were used to adsorb copper ions in an aqueous solution in a batch system, and the maximum adsorption was found to occur at pH 5.5 ± 0.1. The adsorption equilibrium data fitted the Langmuir isotherm equation reasonably well, with a maximum adsorption capacity of 10.41 mg/g. A pseudo second-order model could best describe the adsorption kinetics, and the derived activation energy was 26.92 kJ/mol. The optimum condition to desorb Cu^{2+} from $NH_2/SiO_2/Fe_3O_4$ was provided by a solution with 0.1 mol/L HNO_3.

Key words: magnetic adsorbent; SiO_2; amine; adsorb; copper ion

DOI: 10.1016/S1001-0742(10)60371-3

Citation: Lin Y, Chen H, Lin K, Chen B, Chiou C, 2011. Application of magnetic particles modified with amino groups to adsorb copper ions in aqueous solution. *Journal of Environmental Sciences*, 23(1): 44–50.

Introduction

The removal of heavy metals from wastewater is one of the most important issues due to adverse effects that such metals have on human health and the environment (Nuhoglu and Oguz, 2003). Traditional metal ion treatment processes included chemical precipitation, ion exchange, electrolysis, reverse osmosis, adsorption, etc. Among these treatment methods, adsorption is considered to be an economical, efficient, and promising method for treating metal-ion-contaminated wastewater (Ekmekyapar et al., 2006). Nowadays, most adsorbents developed for the removal of heavy metal ions rely on the interaction of the metal ions with the functional groups present on the surfaces of the adsorbents, and hence, the functional groups play an important role in determining the effectiveness, capacity, selectivity, and reusability of these adsorbents (Prasad and Saxena, 2004; Li and Bai, 2005; Li et al., 2005; Liu et al., 2005). Amine groups have been found to be one of the most efficient functional groups for heavy metal ion removal (Chanda and Rempel, 1995; Ghoul et al., 2003; Gupta et al., 2004), and various adsorbents with amine functional groups have been developed from natural biopolymers (Jin and Bai, 2002) or from synthetic polymers that are subsequently immobilized by the amine groups (Atia et al., 2003; Bayramoglu and Arica, 2005; Deng et al., 2003; Yantasee et al., 2004). The adsorption mechanisms have generally been attributed to the formation of complexes between the amine groups present on the adsorbents and the metal ions to be removed (Deng et al., 2003; Yantasee et al., 2004).

An innovative technology involving solid-liquid phase separation, and which has gained attention, employs adsorbents with magnetic properties. Magnetic separation is now widely used in the fields of medicine, diagnostics, molecular biology (Pankhurst et al., 2003), bioinorganic chemistry, and catalysis (Martin and Mitchell, 1998). Furthermore, magnetic separation method is also beneficial with regard to the environment because it does not result in the production of contaminants such as flocculants (Chang and Chen, 2005; Hu et al., 2005). Conventional magnetic adsorbents are generally commercial carriers made of magnetite particles modified with polymer (Butterworth et al., 2001; Albornoz et al., 2004) or organosilane (Liu et al., 2004), in which suitable functional groups are present on the adsorbent surface.

In this study, a magnetic adsorbent was developed for the adsorption of metal ions. The adsorbents were synthesized by the surface modification of Fe_3O_4 with SiO_2 and N-[3-(trimethoxysilyl)propyl]-ethylenediamine (TPED) containing amino functional groups. These amine

* Corresponding author. E-mail: cschiou@niu.edu.tw

magnetic adsorbents were characterized by X-ray diffraction (XRD), vibrating sample magnetometry (VSM), Brunauer-Emmett-Teller (BET), surface area measurements, UV-Vis spectroscopy, and Fourier transform infrared (FT-IR) spectroscopy. Further, their adsorption behavior and mechanism were examined under various conditions by using copper ions as the model metal contaminant.

1 Materials and methods

1.1 Materials

Magnetite (Fe_3O_4, particle size < 5 μm) and sodium silicate were obtained from Sigma-Aldrich (USA). N-[3-(trimethoxysilyl)propyl]-ethylenediamine, (TPED, $C_8H_{22}N_2O_3Si$), $CuNO_3{\cdot}3H_2O$, and 4-nitrobenzaldehyde of high quality were obtained from Acros Organics (USA) and used without any further purification. All other chemicals were of the reagent grade.

1.2 Instruments

The functional groups of the synthesized adsorbents were confirmed by using an FT-IR spectrometer (Spectrum 100, Perkin Elmer, USA). The specific surface area and pore diameter of the adsorbents were measured by the (BET) method using a particle size analyzer (ASAP 2000C, Micromeritics, USA). The magnetic behavior was analyzed by using a vibrating sample magnetometer (Lake Shore 7407, Lake Shore, USA). The crystal lattice structure of the material was determined by XRD (Theta Probe, Thermo Scientific, UK). The concentration of metal ions in the solution was analyzed by using a flame atomic absorption spectrophotometer (AA932, GBC, Australia).

1.3 Synthesis of adsorbents

1.3.1 Silica-coated magnetite (SiO_2/Fe_3O_4)

A total of 1.08 L of an aqueous solution containing 20 g of magnetite (Fe_3O_4) particles was held in a 2 L beaker at 90°C; its pH was maintained at 9.5 with 0.1 mol/L NaOH, while it was being stirred by a mechanic stirrer. An appropriate amount of sodium silicate was dissolved in 100 mL of deionized water, and the resulting solution was mixed with the above aqueous solution of magnetite. The pH of this mixture was adjusted to 6 by using 2.5 mol/L H_2SO_4, and the mixture was then maintained at 90°C for 30 min under mechanical stirring. Silica coating was applied by the aggregation of silicic acid monomer to form a gel by titration of the silicate solution with sulfuric acid (Iler, 1979). Finally, the reacted magnetite were collected and washed several times with deionized water until the pH of the water collected after washing the adsorbents became approximately 7. The prepared adsorbents were then dried at 105°C for 8 hr and stored in desiccators until further use in the following experiments.

1.3.2 Amine-modified silica magnetite

Ten grams of SiO_2/Fe_3O_4 was reacted with N-[3-(trimethoxysilyl)-propyl]ethylenediamine in 500 mL of refluxing toluene under N_2 for 24 hr. The resulting adsorbent was filtrated and washed by soxlet extraction with ethanol, and then this synthetic adsorbents was followed by drying at 60°C in vacuum. The dry adsorbent was stored in a sealed bottle for further use.

1.4 Adsorption experiments

Adsorption of Cu^{2+} from aqueous solutions was investigated in batch experiments. Effects of pH (3.0–9.0), kinetic experiments (0–2 hr), adsorption isotherm (50–150 mg/L initial Cu^{2+} concentration), and thermodynamic studies (298–328 K) on adsorption were studied. All the adsorption isotherm experiments were carried out at 298 K, in which pH was maintained at 5.5 ± 0.1, the adsorbent concentration was kept constant at 0.5 g in a 50 mL solution, initial Cu^{2+} concentration was in the range from 50 to 150 mg/L, and the equilibrium time was considered as 24 hr. After adsorption reached the equilibrium, the adsorbent was separated via an external magnetic field.

1.5 Desorption experiments

The experiments for desorption efficiency were carried out with dilute HNO_3 solutions in the concentration range of 0.01–2 mol/L. A 0.5 g of the $NH_2/SiO_2/Fe_3O_4$ adsorbent adsorbed with about 10 mg/g copper ions were placed into 100 mL of a HNO_3 solution with thermostatic shaking and the desorption was allowed for a time period up to 24 hr. The desorption efficiency (DE) was determined using the following Eq. (1):

$$\mathrm{DE} = \frac{C \times V}{q \times m} \times 100\% \tag{1}$$

where, C (mg/L) is the concentration of copper ions in the desorption solution, V (L) is the volume of the desorption solution, q (mg/g) is the amount of copper ions adsorbed on the adsorbents before desorption experiment, and m (g) is the amount of the adsorbent used in the desorption experiments.

2 Results and discussion

2.1 Characterization of magnetic adsorbent

2.1.1 FT-IR

The FT-IR spectra of Fe_3O_4, SiO_2/Fe_3O_4, and the prepared magnetic amine adsorbent ($NH_2/SiO_2/Fe_3O_4$) are shown in Fig. 1. The figure exhibits two basic characteristic peaks of these three adsorbents at approximately 3300 cm^{-1} (O–H stretching) and 550 cm^{-1} (Fe–O vibration), which were attributed to the presence of FeOH in Fe_3O_4 (Phan and Jones, 2006). The peaks at 1100 cm^{-1} were attributed to the Si–O–Si bond stretching of SiO_2/Fe_3O_4 and $NH_2/SiO_2/Fe_3O_4$. This result confirms that SiO_2 was successfully coated on Fe_3O_4. Furthermore, in Fig. 1, the peaks of $NH_2/SiO_2/Fe_3O_4$ are located at 1496 cm^{-1} (C–H stretching) and 1643 cm^{-1} (N–H bending); these peaks indicated that TPED had been bonded with the surface of SiO_2/Fe_3O_4. Amine compound also possesses a characteristic peak around 3300 cm^{-1} (N–H stretching)

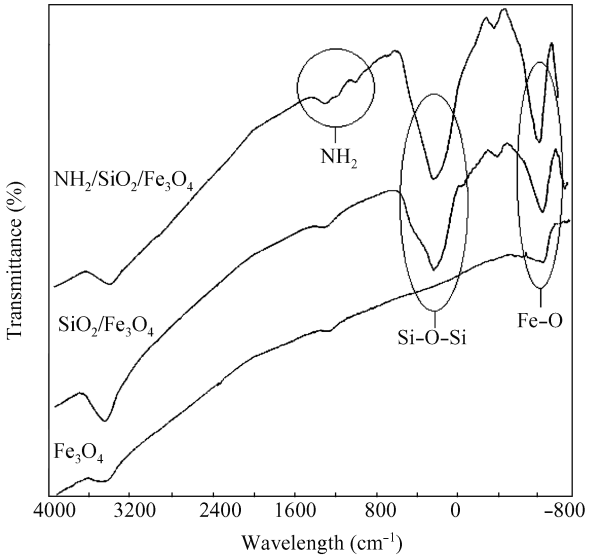

Fig. 1 FT-IR spectra of Fe_3O_4, SiO_2/Fe_3O_4, and $NH_2/SiO_2/Fe_3O_4$.

in an IR spectrum, but this peak was interfered from O–H stretching absorbance. In addition, the characteristic peaks of C–H stretching and N–H bending for the synthesized $NH_2/SiO_2/Fe_3O_4$ were too weak to be observed clearly. Therefore, another analytical method, UV absorbance, was employed to prove that the amine group had bonded on the surface of SiO_2/Fe_3O_4.

2.1.2 UV absorbance

The amine groups anchored on the support surface could be determined by a UV colorimetric method that involved their reaction with a UV-sensitive reagent (4-nitrobenzaldehyde) (Campo et al., 2005). This reaction between amine and aldehyde groups under anhydrous conditions generates an imine group that may be hydrolyzed back to the precursors in a known volume of water to produce 4-nitrobenzaldehyde whose absorbance (282 nm) can be measured by UV spectroscopy. The number of hydrolyzed aldehyde molecules is proportional to the number of imine molecules present. Figure 2 shows the results of colorimetric analyses performed on Fe_3O_4, SiO_2/Fe_3O_4, and $NH_2/SiO_2/Fe_3O_4$. It is clear that the UV absorbance at a wavelength of 282 nm in the case of $NH_2/SiO_2/Fe_3O_4$, containing an amine group, was larger than that in the case of Fe_3O_4 and SiO_2/Fe_3O_4. The UV absorbences of Fe_3O_4 and SiO_2/Fe_3O_4, without an amine group, were almost zero. These results also confirmed that the surface of the synthesized $NH_2/SiO_2/Fe_3O_4$ had been modified with amine group.

2.1.3 BET, XRD, VSM

BET surface area measurements indicated that compared to the Fe_3O_4 core, the surface area of SiO_2/Fe_3O_4 significantly increased from 18.06 to 114.02 m^2/g. This may be due to the coating of SiO_2 formed on Fe_3O_4 by sodium silicate method containing porous surface. When SiO_2/Fe_3O_4 was modified with the amine group, the BET surface area decreased to 72.89 m^2/g. This decrease in the surface area may be attributed to the possibility that

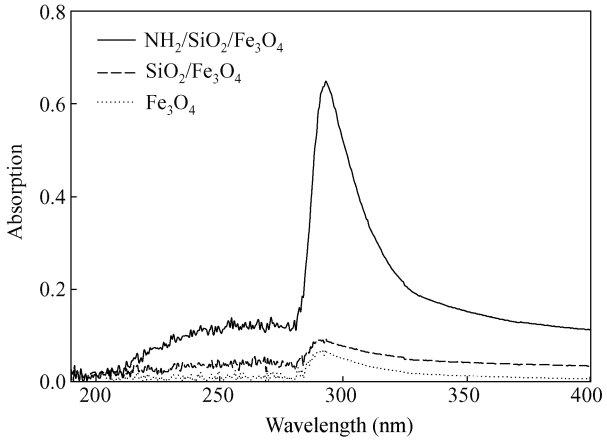

Fig. 2 UV colorimetric analyses of amine groups with 4-nitrobenzaldehyde performed on Fe_3O_4, SiO_2/Fe_3O_4, and $NH_2/SiO_2/Fe_3O_4$. UV absorbance at wavelength 282 nm.

the pores of SiO_2 were partially covered by the modified amino compound (TPED).

According to the database of Joint Committee on Powder Diffraction Standards (JCPDS), the XRD pattern of a standard Fe_3O_4 crystal with spinel structure has six characteristic peaks at 2θ = 30.1°, 35.5°, 43.1°, 53.4°, 57.0°, and 62.6° that are attributed to the (2 2 0), (3 1 1), (4 0 0), (4 2 2), (5 1 1), and (4 4 0) phases of Fe_3O_4, respectively. It is apparent that as shown in Fig. 3, the analysis results of the starting material Fe_3O_4, SiO_2/Fe_3O_4, and $NH_2/SiO_2/Fe_3O_4$ fitted the pattern exhibited by standard magnetite. Therefore, it can be concluded that the magnetite modified with SiO_2 and TPED is also of spinel structure and that these modifications don't cause a phase change in Fe_3O_4.

The magnetic properties of the $NH_2/SiO_2/Fe_3O_4$ and Fe_3O_4 cores were measured by VSM (Fig. 4). The mass saturation magnetization (Ms) of Fe_3O_4 was found to be 61.8 emu/g, which is in good agreement with the value in literature (Shi et al., 2006). The plots shown in Fig. 4 exhibited a change in Ms of the particles after the incorporation of a NH_2/SiO_2 shell. A decrease in Ms from 61.8 to 57.2 emu/g was observed in the case

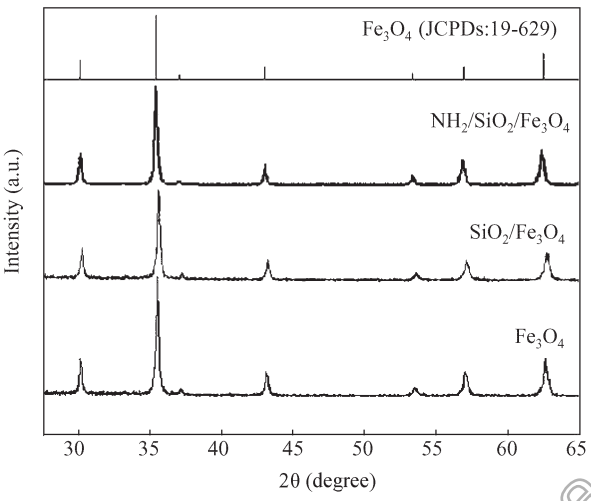

Fig. 3 XRD spectra of Fe_3O_4, SiO_2/Fe_3O_4, and $NH_2/SiO_2/Fe_3O_4$.

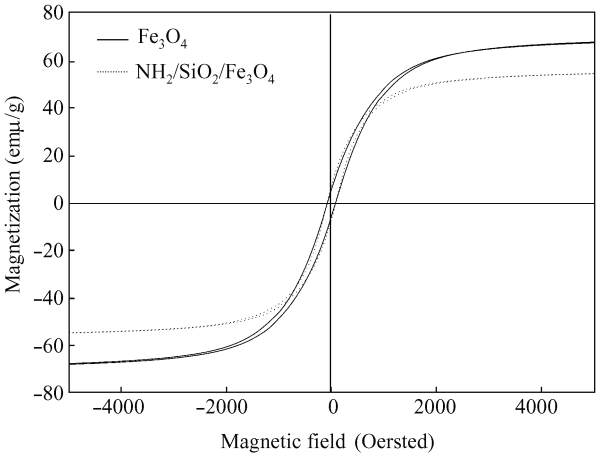

Fig. 4 Magnetization versus applied magnetic field for Fe_3O_4 and $NH_2/SiO_2/Fe_3O_4$.

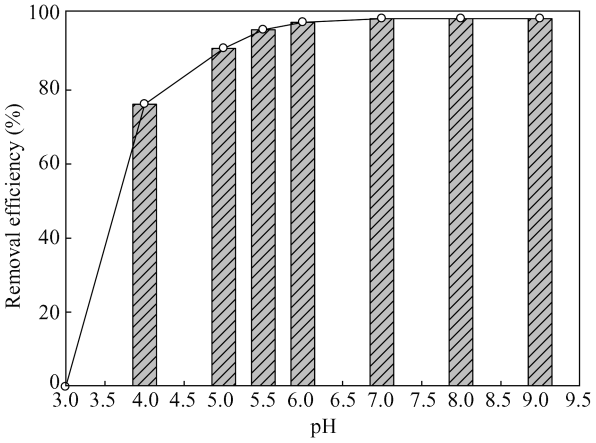

Fig. 5 Effect of solution pH on copper ion adsorption onto the $NH_2/SiO_2/Fe_3O_4$ adsorbent. Experimental conditions: initial concentration of Cu^{2+} ($C_{Cu^{2+},0}$) = 50 mg/L, $NH_2/SiO_2/Fe_3O_4$ 10 g/L, reaction time = 24 hr, temperature = 298 K. The pH value of the solution was controlled by adding 0.05 mol/L H_2SO_4 and 0.1 mol/L NaOH. Removal efficiency (%) = $(1 - \frac{C_{Cu^{2+},f}}{C_{Cu^{2+},0}}) \times 100\%$, where $C_{Cu^{2+},f}$ is the final concentration of Cu^{2+}.

of $NH_2/SiO_2/Fe_3O_4$. This decrease was ascribed to the contribution of the nonmagnetic NH_2/SiO_2 shell to the total mass of the particles. This observation is similar to that made in another study, in which the attached gold shell was found to lower the saturation magnetization of magnetite particles (Vestal and Zhang, 2002). The results in Fig. 4 also indicated that the prepared particles exhibited a paramagnetic behavior at room temperature (Pankhurst et al., 2003; Xu et al., 2008).

2.2 Effect of pH on adsorption of copper ions

At a high solution pH, copper ions precipitated as $Cu(OH)_{2(s)}$, and the amount of copper species present in the aqueous solution in the forms of Cu^{2+}, $Cu(OH)^+$, $Cu(OH)_2^0$, $Cu(OH)_3^-$, and $Cu(OH)_4^{2-}$ vary with the solution pH (Kumar et al., 2007). These copper ions, except Cu^{2+}, interfere with the ability of $NH_2/SiO_2/Fe_3O_4$ to adsorb copper ions. Furthermore, the solution pH value determines whether or not the amine groups on the synthetic magnetic adsorbent are protonated. Protonated amine groups cannot adsorb Cu^{2+}. Figure 5 shows the performance of the $NH_2/SiO_2/Fe_3O_4$ adsorbent in adsorbing copper ions at different solution pH values. The result revealed that the adsorption behavior of $NH_2/SiO_2/Fe_3O_4$ with Cu^{2+} is strongly pH-dependent. At solution pH = 3, the adsorption efficiency of Cu^{2+} by $NH_2/SiO_2/Fe_3O_4$ was nearly zero. At low solution pH values (high acidic environment), a relatively high concentration of protons would strongly compete with copper ions for amine sites, and thus, the adsorption of copper ions was significantly decreased. On the other hand, the protonation of the amine groups would lead to strong electrostatic repulsion of the copper ions to be adsorbed. As a result, it became difficult for copper ions to come in close contact with the adsorbent surface and be adsorbed thereon; this resulted in poor adsorption performance at solution pH = 3.

At higher solution pH values of 4–6, the competition of protons with copper ions for the amine groups became less significant, and more of the amine groups existed in their neutral form, which reduced the electrostatic repulsion of copper ions; furthermore, the unpaired electrons of amine groups could also create coordinate bonds with copper ions. Hence, more copper ions could be adsorbed onto the surfaces of $NH_2/SiO_2/Fe_3O_4$, resulting in the observed increase in Cu^{2+} adsorption on the adsorbent. Fig. 5 also indicated a complete removal of Cu^{2+} from the solution when the solution pH value exceeded 6.5. This is attributed to Cu^{2+} began to precipitate as $Cu(OH)_2$. Therefore, copper ions were removed by both adsorption and precipitation when the solution pH value exceeded 6.5 (Ko et al., 2003). As a result, the optimum pH for Cu^{2+} adsorption by $NH_2/SiO_2/Fe_3O_4$ was found to be in the pH range 5–6, and all further experiments were carried out at solution pH = 5.5.

2.3 Adsorption isotherms of copper ions

The equilibrium isotherms for the adsorption of copper ions by $NH_2/SiO_2/Fe_3O_4$ were conducted at pH 5.5, 298 K, 10 g/L adsorbent dose, and five initial Cu^{2+} concentrations: 50, 75, 100, 125, and 150 mg/L. The equilibrium data are shown in Table 1 and fitted by Langmuir and Freundlich isotherm equations (Wong et al., 2003). The Langmuir equation can be expressed as following Eq. (2).

$$\frac{C_e}{q_e} = \frac{C_e}{q_m} + \frac{1}{q_m K_L} \tag{2}$$

Table 1 Adsorption isotherm results for copper ion adsorption on $NH_2/SiO_2/Fe_3O_4$ adsorbents

Initial concentration (mg/L)	Equilibrium concentration (C_e, mg/L)	Adsorption quantity (mg/g)
25	1.21	2.38
50	3.39	4.66
75	6.12	6.89
100	19.06	8.09
125	34.76	9.02

Solution pH 5.5; $NH_2/SiO_2/Fe_3O_4$ 10 g/L; reaction time 24 hr; temperature 298K.

where, q_e (mg/g) is the equilibrium adsorption capacity of copper ions on the adsorbent; C_e (mg/L), the equilibrium copper ion concentration in solution; q_m (mg/g), the maximum capacity of adsorbent; and K_L (L/mg), the Langmuir adsorption constant. The linear form of Freundlich equation can be represented as following Eq. (3).

$$\log q_e = \log k_F + \frac{1}{n}\log C_e \quad (3)$$

where, K_F (L/mg) is the Freundlich constant, and n is the heterogeneity factor.

Table 2 shows the values of q_m and K_L, determined from the slope and intercept of the linear plots of C_e/q_e versus C_e, and the values of K_F and $1/n$, determined from the slope and intercept of the linear plot of $\ln q_e$ versus $\ln C_e$. The correlation coefficients of the Langmuir and Freundlich isotherms were found to be 0.9933 and 0.9585, respectively. This result revealed that the data were fitted better by the Langmuir equation than by the Freundlich equation. Fitting of the Langmuir isotherm indicates monolayer coverage of Cu^{2+} on the surface of $NH_2/SiO_2/Fe_3O_4$ during adsorption. The maximum monolayer copper uptake (q_m) was found to be 11.24 mg/g.

Table 2 Parameter values of Langmuir and Freundlich models fitting to the experimental results in Table 1 for copper ion adsorption on the $NH_2/SiO_2/Fe_3O_4$ adsorbents

	Langmuir		Freundlich		
q_m (mg/g)	K_L (L/mg)	R^2	n	K_F	R^2
10.41	0.0376	0.9956	2.63	1.53	0.8906

2.4 Adsorption kinetics

Figure 6 shows the effect of contact time on the adsorption of Cu^{2+} by $NH_2/SiO_2/Fe_3O_4$ from a solution under different temperatures. The adsorption occurred rapidly during the early stages of the adsorption reaction, which was probably due to the abundant availability of active sites on the adsorbents. However, with a gradual decrease in the number of active sites in the bulk solution, the adsorption reaction became slower. Figure 6 also reveals that high solution temperature slowed down the adsorption kinetic; this implies that the adsorption behavior was exothermic. Adsorption kinetic data are often analyzed using two commonly used kinetic models, namely, the pseudo first-order and pseudo second-order kinetic models that can be expressed in their linearized forms as Eqs. (4) and (5) respectively (Mellah et al., 2006):

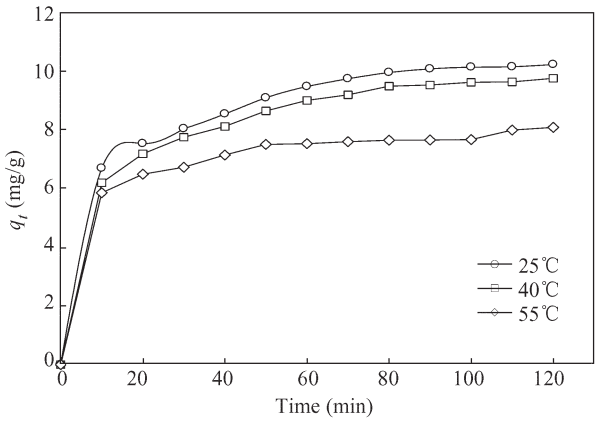

Fig. 6 Dependence of adsorption of Cu^{2+} by $NH_2/SiO_2/Fe_3O_4$ on time at various temperatures. Experimental conditions: $C_{Cu_0^{2+}}$ = 125 mg/L, $NH_2/SiO_2/Fe_3O_4$ 10 g/L, pH 5.5 ± 0.1. The pH value of the solution was controlled by adding 0.05 mol/L H_2SO_4 and 0.1 mol/L NaOH. q_t (mg/g) is the adsorption uptake at time t (min).

$$\log(q_e - q_t) = \log q_e - \frac{k_1}{2.303}t \quad (4)$$

$$\frac{t}{q_t} = \frac{1}{k_2 q_e^2} + \frac{1}{q_e}t \quad (5)$$

where, q_t (mg/g) is the adsorption uptake at time t (min); q_e (mg/g) is the adsorption capacity at adsorption equilibrium; and k_1 (min^{-1}), and k_2 (g/(mg·min)) are the kinetics rate constants for the pseudo first-order and the pseudo second-order models, respectively. Equations (4) and (5) were fitted to the experimental data as shown in Fig. 6, and the calculated model parameters are given in Table 3. The results clearly indicate that the adsorption kinetics closely followed the pseudo second-order kinetic model rather than the pseudo first-order kinetic model, suggesting that the adsorption process was very fast, probably dominated by a chemical adsorption phenomenon. High solution temperature is also clearly found to result in slow adsorption kinetics (smaller values for k_2; Table 3). Moreover, the temperature dependence of the kinetic parameter k_2 in Table 3 can be described by the Arrhenius equation (Eq. (6)).

$$\ln k = \ln A - E_a/RT \quad (6)$$

where, A, E_a, T, and R are the frequency factor, activation energy, temperature (K), and gas constant, respectively. By plotting $\ln k_2$ against $1/T$, the reaction temperatures are determined as 25, 40, and 55°C, which give E_a of 26.92 kJ/mol.

2.5 Desorption and repeated use

Good desorption performance of an adsorbent is important for its potential practical applications. The results shown in Figure 5 revealed that the $NH_2/SiO_2/Fe_3O_4$ adsorbent did not adsorb copper ions significantly at solution pH = 3, suggesting that the adsorbed copper ions may be possibly desorbed in an acidic solution with a low solution pH value. Therefore, HNO_3 solutions with different concentrations were examined in a desorption study. Figure 7 shows the desorption efficiency obtained at various HNO_3 concentrations in desorption solutions. It is

Table 3 Parameter values of the kinetics models fitting to the experimental results in Fig. 6 for copper ion adsorption on the $NH_2/SiO_2/Fe_3O_4$ adsorbent.

Temperature (°C)	R^2		Rate constant (k_2) (g/(mg·min))	Activated energy (E_a) (kJ/mole)
	First order	Second order		
25	0.964	0.991	0.0010	
40	0.976	0.996	0.0018	26.92
55	0.882	0.994	0.0029	

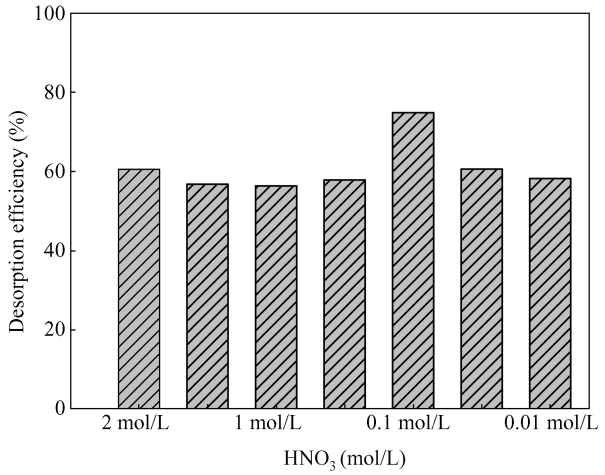

Fig. 7 Desorption efficiency of copper ions from the $NH_2/SiO_2/Fe_3O_4$ adsorbent in solutions with different HNO_3 concentrations. Experimental conditions: $NH_2/SiO_2/Fe_3O_4$ 5 g/L, reaction time 24 hr, T 298 K.

interesting to note that the maximum desorption efficiency was achieved at HNO_3 concentration of 0.1 mol/L, and any higher or lower HNO_3 concentrations resulted in lower desorption efficiencies. In order to explain this, one may assume that the reactions taking place in acidic desorption solutions can be given by the following Reactions (7) and (8) (Liu et al., 2006):

$$SiO_2/Fe_3O_4\text{-}NH_2 \cdots Cu^{2+} + H^+ \Longleftrightarrow SiO_2/Fe_3O_4\text{-}NH_3^+ + Cu^{2+} \quad (7)$$

$$SiO_2/Fe_3O_4\text{-}NH_2 + H^+ \Longleftrightarrow SiO_2/Fe_3O_4\text{-}NH_3^+ \quad (8)$$

In a solution with HNO_3 concentration exceeding 0.1 mol/L, the high concentration of H^+ will shift both Reactions (7) and (8) to the right-hand side and more $SiO_2/Fe_3O_4\text{-}NH_3^+$ will be generated. However, the generation of $SiO_2/Fe_3O_4\text{-}NH_3^+$ will favor the reverse reaction of Reaction (7) to the left-hand side, thus not favoring the desorption of copper ions from an adsorbent. Therefore, when the concentration of HNO_3 in the desorption solution became greater than 0.1 mol/L, the reverse reaction in Reaction (7) actually started to hinder the desorption of copper ions from the adsorbents, resulting in a reduced desorption efficiency. On the other hand, a concentration lower than 0.1 mol/L HNO_3 (lower H^+ concentration) in the desorption solution may be insufficient to drive Reaction (7) to the right-hand side for the desorption of copper ions; thus leading to observed desorption efficiencies lower than that at 0.1 mol/L HNO_3 concentration.

In order to determine the reusability of $NH_2/SiO_2/Fe_3O_4$, adsorption-desorption cycles were repeated three times by using the same amine magnetic adsorbent. The adsorption capacity of the recycled $NH_2/SiO_2/Fe_3O_4$ exhibited a loss of about 13.6% in the third cycle. The loss of the adsorption capacity may be attributed to the detachment of the silica coating from the magnetite surface during the recycling processes, which is evidence by the presence of dissolved silicate in the adsorption reaction solution. Further investigations are necessary to develop strategies to prevent the separation of the coating from the core surface and maintain the function of the synthetic magnetic adsorbent.

3 Conclusions

Amine-functionalized silica magnetite has been synthesized using TPED as the surface modification agent. The following are the results of this study.

1. The optimum solution pH for Cu^{2+} adsorption by $NH_2/SiO_2/Fe_3O_4$ was found to be in the range of 5–6.

2. The equilibrium data of copper ion adsorption by $NH_2/SiO_2/Fe_3O_4$ were in good agreement with the Langmuir model with a maximum monolayer copper uptake (q_m) of 10.41 mg/g.

3. Copper ions removed by $NH_2/SiO_2/Fe_3O_4$ followed second-order kinetics, and high solution temperature resulted in slow adsorption kinetics. The Arrhenius equation yielded E_a of 26.92 kJ/mol.

4. The optimum condition to desorb Cu^{2+} from $NH_2/SiO_2/Fe_3O_4$ is with 0.1 mol/L HNO_3.

References

Albornoz C, Sileo E E, Jacobo S E, 2004. Magnetic polymers of maghemite (g-Fe_2O_3) and polyvinyl alcohol. *Physica B: Condensed Matter*, 354: 149–153.

Atia A A, Donia A M, Abou-El-Enein S A, Yousif A M, 2003. Studies on uptake behavior of copper(II) and lead(II) by amine chelating resins with different textural properties. *Separation & Purification Technology*, 33: 295–301.

Bayramoglu G, Arica M Y, 2005. Ethylenediamine grafted poly (glycidyl-methacrylate-co-methylmethacrylate) adsorbent for removal of chromate anions. *Separation & Purification and Technology*, 45: 192–199.

Butterworth M D, Illum L, Davis S S, 2001. Preparation of ultrafine silica- and PEG-coated magnetite particles. *Colloids and Surfaces A: Physicochemical and Engineering Aspects*, 179: 93–102.

Campo A, Sena T, Lellouchec J P, Bruce I J, 2005. Multifunctional magnetite and silica-magnetite nanoparticles: Synthesis, surface activation and applications in life sciences. *Journal of Magnetism and Magnetic Materials*, 293: 33–40.

Chanda M, Rempel G L, 1995. Polyethyleneimine gel-coat on silica: high uranium capacity and fast kinetics of gel-coated resin. *Reactive Polymers*, 25: 25–36.

Chang Y C, Chen D H, 2005. Preparation and adsorption properties of monodisperse chitosan-bound Fe_3O_4 magnetic nanoparticles for removal of Cu(II) ions. *Journal of Colloid Interface Science*, 283: 446–451.

Deng S, Bai R B, Chen J P, 2003. Aminated polyacrylonitrile fibers for lead and copper removal. *Langmuir*, 19: 5058–5064.

Ekmekyapar F, Aslan A, Kemal Bayhan Y, Cakici A, 2006. Biosorption of copper(II) by nonliving lichen biomass of Cladonia rangiformis hoffm. *Journal of Hazardous Materials, B*, 137: 293–298.

Ghoul M, Bacquet M, Morcellet M, 2003. Uptake of heavy metals from synthetic aqueous solutions using modified PEI-silica gels. *Water Research*, 37: 729–734.

Gupta R K, Singh R A, Dubey S S, 2004. Removal of mercury ions from aqueous solutions by composite of polyaniline with polystyrene. *Separation & Purification Technology*,

38: 225–232.

Hu J, Chen G, Lo I M C, 2005. Removal and recovery of Cr(VI) from wastewater by maghemite nanoparticles. *Water Research*, 39: 4528–4536.

Iler R K, 1979. The Chemistry of Silica. John Wiley & Sons, New York, USA.

Jin L, Bai R B, 2002. Mechanisms of lead adsorption on chitosan/PVA hydrogel beads. *Langmuir*, 18: 9765–9770.

Ko D C K, Porter J F, McKay G, 2003. Mass transport model for the fixed bed sorption of metal ions on bone char. *Industrial & Engineering Chemistry Research*, 42: 3458–3469.

Kumar G P, Kumar P A, Chakraborty S, Ray M, 2007. Uptake and desorption of copper ion using functionalized polymer coated silica gel in aqueous environment. *Separation and Purification Technology*, 57: 47–56.

Li N, Bai R B, 2005. Copper adsorption on chitosan-cellulose hydrogel beads: behaviors and mechanisms. *Separation & Purification Technology*, 42: 237–247.

Li N, Bai R B, Liu C, 2005. Enhanced and selective adsorption of mercury ions on chitosan beads grafted with polyacrylamide via surface-initiated atom transfer radical polymerization. *Langmuir*, 21: 11780–11787.

Liu C C, Wang M K, Li Y S, 2005. Removal of nickel from aqueous solution using wine processing waste sludge. *Industrial & Engineering Chemistry Research*, 44: 1438–1445.

Liu C K, Bai R, Hong L, 2006. Diethylenetriamine-grafted poly(glycidyl methacrylate) adsorbent for effective copper ion adsorption. *Journal of Colloid and Interface Science*, 303: 99–108.

Liu X, Ma Z, Xing J, Liu H, 2004. Preparation and characterization of amino-silane modified superparamagnetic silica nanospheres. *Journal of Magnetism and Magnetic Materials*, 270: 1–6.

Martin C R, Mitchell D T, 1998. Nanomaterials in analytical chemistry. *Analytical Chemistry*, 70(9): 322A–327A.

Mellah A, Chegrouche S, Barkat M, 2006. The removal of uranium(VI) from aqueous solutions onto activated carbon: Kinetic and thermodynamic investigations. *Journal of Colloid and Interface Science*, 296: 434–441.

Nuhoglu Y, Oguz E, 2003. Removal of copper(II) from aqueous solutions by biosorption on the cone biomass of Thuja orientalis. *Process Biochemistry*, 38: 1627–1631.

Phan N T S, Jones C W, 2006. Highly accessible catalytic sites on recyclable organosilane-functionalized magnetic nanoparticles: An alternative to functionalized porous silica catalysts. *Journal of Molecular Catalysis A: Chemical*, 253: 123–131.

Pankhurst Q A, Connolly J, Jones S K, Dobson J, 2003. Application of magnetic nanoparticles in biomedicine. *Journal of Physical Data*, 36: R167–R181.

Prasad M, Saxena S, 2004. Sorption mechanism of some divalent metal ions onto low-cost mineral adsorbent. *Industrial & Engineering Chemistry Research*, 43: 1512–1522.

Shi Y L, Qiu W, Zheng Y, 2006. Synthesis and characterization of a POM-based nanocomposite as a novel magnetic photocatalyst. *Journal of Physics and Chemistry of Solids*, 67: 2409–2418.

Vestal C R, Zhang Z J, 2002. Atom transfer radical polymerization synthesis and magnetic characterization of $MnFe_2O_4$/polystyrene core/shell nanoparticles. *Journal of American Chemical Society*, 124: 14312–14313.

Wong Y C, Szeto Y S, Cheung W H, Mckay G, 2003. Equilibrium studies for acid dye adsorption onto chitosan. *Langmuir*, 19: 7888–7894.

Xu J, Ao Y, Fu D, Yuan C, 2008. Low-temperature preparation of anatase titania-coated magnetite. *Journal of Physics and Chemistry of Solids*, 69: 1980–1984.

Yantasee W, Lin Y, Fryxell G E, Alford K L, Busche B J, Johnson C D, 2004. Selective removal of copper(II) from aqueous solutions using fine-grained activated carbon functionalized with amine. *Industrial & Engineering Chemistry Research*, 43: 2759–2764.